The switch of behaviour of sized papers during liquid drop impaction

Dushmantha Kannangara, Hailong Zhang and Wei Shen*

Keywords: Liquid drop impact and recoil, sized paper surface, liquid-paper interaction

Abstract

The impact and recoil of water drops on several flat and macroscopically smooth model surfaces and a sized commercial paper were studied over a range of drop velocities using a high speed CCD camera. Results of the water drop impact and recoil obtained from the model hydrophobic and hydrophilic surfaces were in agreement with observations reported previously. The maximum drop spreading diameter at the impaction was found to be dependent upon the initial drop kinetic energy and the extent of drop recoil from the substrates after impaction was found to be much weaker for hydrophilic substrates than for hydrophobic substrates. The sized papers, however, showed an interesting switch of behavior in the process of water drop impact and recoil. The sized paper was found to behave like a hydrophobic substrate as water drop impacts on it, but like a hydrophilic substrate as water drop recoils. Implications of this phenomenon were discussed in the context of inkjet print quality and of the surface conditions of the sized paper. Atomic force microscopy (AFM) was used to probe fibres on a sized filter paper surface under water. The AFM data showed that water interacted strongly with the fibre surface even though the paper was heavily sized. Results of this study are very useful to the understanding of inkjet ink droplet impaction on paper surface which sets the initial condition for ink penetration into paper after impaction.

Introduction

Phenomena associated with a liquid drop impaction on a solid surface and the spreading thereafter can be seen in many industrial applications. Spreading of herbicides on leafs, spray painting and inkjet printing are just a few examples to mention. Liquid drop impaction on impervious and macroscopically smooth solid surfaces of hydrophilic and hydrophobic natures has been studied by many researchers [1-5]. Some mathematical modeling approaches were explored in these studies for predicting the maximum diameter of the forced spreading of a liquid drop when impacting on a smooth solid surface and the minimum diameter of the drop-surface contact area when the drop recoiled after the impaction. The basic consideration common to all these studies was the conservation of energy. The impaction of water drops on hydrophilic and hydrophobic smooth solid surfaces was summarized by Park *et al*. [1]. Water drop impact on hydrophilic surfaces has two clear stages: The drop is first forced to spread to the maximum diameter at the impaction and then settles on the final equilibrium drop diameter. On the other hand, the water drop impact on hydrophobic surfaces has four

* Australian Pulp and Paper Institute (APPI), Department of Chemical Engineering, Monash University, Clayton Campus, Vic. 3800, Australia.
Email: wei.shen@eng.monash.edu.au

stages: immediately before impaction, the forced drop spreading to the maximum diameter, drop recoil to its maximum extent, and reaching to the equilibrium.

Impacts of water-based inkjet inks and commercial paper surfaces were also reported [6, 7]. The study by Asai *et al*. [6] also employed the principle of energy conservation, and treating the paper surface as a macroscopically smooth solid surface. These authors reported that the maximum forced spreading of the inkjet droplets was independent upon the characteristics of paper surface [6]. However, paper samples used in this study was not thoroughly characterized.

To understand the spreading and the penetration of inkjet inks into paper, the knowledge of liquid spreading on solid surfaces is important. Liquid spreading on solid surfaces has also been investigated by many authors. Some studies revealed that the kinetics of liquid wetting of smooth solid surfaces could be well characterized by a simple power law [8,9]. Other studies reported that wetting kinetics on rough surfaces could also be described by simple power models [10,11]. However, Apel Paz and Marmur [10] showed that using the simple power model to describe liquid spreading on a rough surface was empirical.

In our laboratory, ink and paper interaction has been a research subject for several years. The primary interest of this investigation was to study the behaviour of a liquid drop in the event of impacting on sized paper surfaces. Empirical observations of inkjet printing trials showed that inkjet printing quality deteriorated badly if ink droplets amalgamated after landing on the paper surface [12]. Such ink droplet amalgamation could be further promoted by ink drop impaction and ink spreading and penetration after impaction. While the ink spreading and penetration into the paper surface has been investigated by many researchers [11,13-15], the liquid (ink) droplet impact on paper surfaces has received relatively less research attention [6,7].

In order to make our research idea clear, it is necessary to also review some literature work on ink and paper interactions. The Washburn equation has been used traditionally as a model to describe the penetration of liquid into a paper [16]. More recent studies showed that the Washburn model gave first order description to the liquid penetration into paper [13]. A microscopic study showed that penetration of water in an unsized paper was via the film flow [15] and the film flow could not be observed from the sized papers [17]. Modaressi and Garnier [11] observed that the interaction of a water droplet and a paper could be described by two sequential phenomena, i.e., the wetting of paper surface by water until a pseudo-equilibrium contact angle was reached, followed by the water drop absorbed into the bulk of paper. The first process does not occur instantaneously, if the paper is sized [11]. Lyne and Aspler [14] also published some empirical data suggesting that a wetting delay might be appropriate to describe the delay between the onset of liquid penetration and the moment of liquid-paper contact was made.

Whereas the liquid penetration studies have provided much information to the understanding of ink-paper interactions in printing, ink droplet impaction to the paper surface also contains useful and relevant information to inkjet printing. Since ink paper interactions consist of two consecutive processes of wetting (spreading) and penetration, drop impaction is likely to affect the spreading process [6]. The status of the ink and paper interaction immediately after the drop impaction may influence the starting condition of the liquid penetration after the drop impaction. In this regard, not only the

forced maximum drop spreading is important, but the maximum retraction and liquid drop recoil are also important. These processes strongly influence the size of the dot an ink droplet makes on the paper surface. Park *et al*. [1] showed, using data obtained from impervious and macroscopically smooth solid surfaces, that the liquid drop contact area with the solid substrates reduced when the drop recoiled after the impaction. These authors also showed that the minimum diameter of this contact area could be correlated with the work of adhesion between the liquid and the solid [1]. The larger the value of work of adhesion, the weaker the liquid drop retraction, and thus, the larger the minimum diameter would be. Asai *et al*. [6], on the other hand, showed that the maximum forced drop spreading diameter on paper surfaces could be correlated only with the Reynolds (*Re*) and Weber (*We*) numbers, and showed no correlation to the characteristics of the papers used. Their results seem to suggest that the paper surface might not be treated as a simple surface.

Characterization of the work of adhesion between liquids and paper using the contact angle methods is rather difficult [18,19]. As a result, the large contact angle for water on cellulose fibre and paper surfaces caused by sizing was interpreted as these substrates being hydrophobized [11,20]. In fact, the interaction between an aqueous solution and cellulose fibres (even strongly sized) is rather extraordinary. It may be not appropriate to describe the heavily sized cellulose fibres simply as hydrophobic, instead, it may be more appropriate to describe the sized fibre surface as a hydrophilic surface with domains of sizing chemicals. These domains of sizing chemicals, however, could not totally cut off the interactions between liquid molecules and the hydrophilic areas of the fibre surface that were not covered by these domains, although the presence of these domains slows down the wetting of the fibre by the aqueous solution by pinning the three-phase contact line. This fact may have a strong influence to the liquid drop spreading and recoiling.

In this study, water drop impactions with hydrophilic and hydrophobic model surfaces, as well as a sized commercial copy paper surface were investigated. Atomic force microscope was also used to conduct an under water study the effect of swelling of heavily sized fibres by water. Results obtained are discussed in the contexts of inkjet printing quality and chemical conditions of the sized paper surface.

Experimental

Materials and reagents

Water (Millipore, 18 MΩ) and Diiodomethane (99%, Aldrich) were used as liquid probes to determine the surface energy of the solid substrates. Surface tension data of these probes obtained from the literature [21] are listed in Table 1.

Table 1: Surface tension (mN/m) values of liquid probes [21]

Liquid	Surface Tension(γ_{lv})	Polar Component(γ^p)	Dispersive Component(γ^d)
Water	72.7	51.1	21.7
Diidomethane	50.8	0.0	50.8

Cellulose acetate (99%, Aldrich) and sodium methoxide (25% in methanol, Aldrich) were used for preparing smooth cellulose film on glass slides. Analytical grade methanol (BDH) and acetone (BDH) were used as solvents for preparing the cellulose film. AKD wax was supplied by Hercules Chemicals Australia Pty Ltd. The wax was re-crystallized in AR grade acetone twice before being used. AR grade n-heptane (99.5%, Ajax) was used to make up AKD–heptane solutions, which were used for solvent sizing of cellulose films.

Teflon sheet (thickness = 0.5 mm) was obtained from Goodfellow (UK). Microscopic glass slides were supplied by Bio Lab, Australia. A commercial copy paper (Reflex) was used as the paper substrate. Reflex copy paper was 80 gsm paper made using predominantly the fully bleached eucalypt kraft pulp under the alkaline condition. The Reflex copy paper was well sized using AKD, its contact angle with water was close to 120º. Both Teflon sheet and glass slides were washed with ample amount of Millipore water followed by rinsing with methanol and acetone. The Teflon sheet and glass slides were dried in an oven at 60˚C after allowing the solvents to evaporate. The dried substrates were used for tests and sample preparation described below.

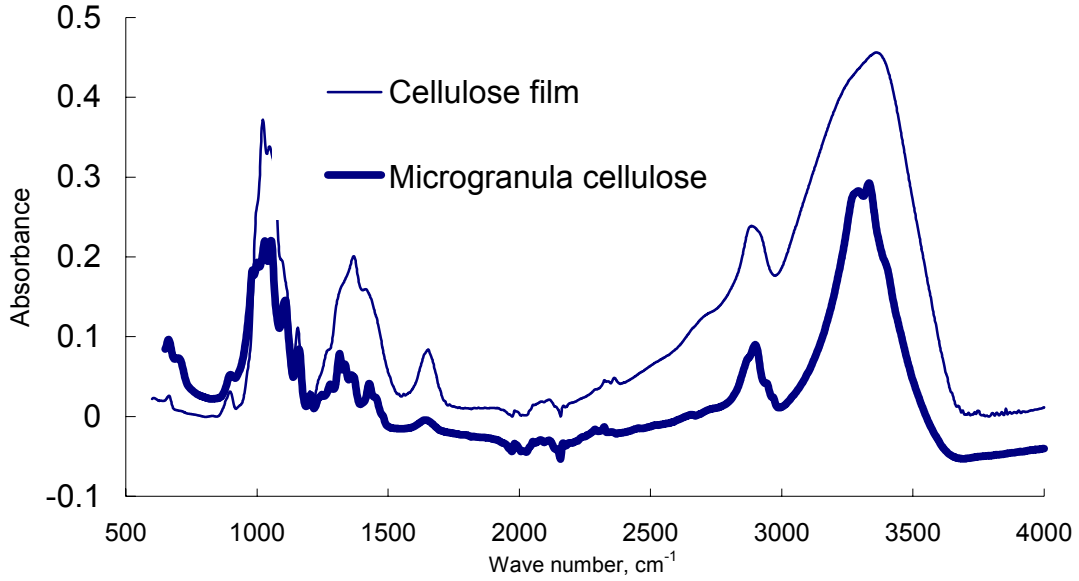

Figure 1. FTIR spectra of (a) cellulose film formed in this study and, (b) microgranular cellulose obtained from Aldrich.

Cellulose film generation on glass slide

A cellulose acetate film was first prepared by slowly dipping a clean microscope slide into a solution of 1% cellulose acetate in acetone (w/w). Upon removal of the slide out of the solution acetone quickly evaporated, leaving a thin and smooth film of cellulose acetate on the glass slide. Cellulose acetate film was then hydrolyzed to form cellulose in 0.5% sodium methoxide (v/v) in methanol for at least 12 hours. The slides were then washed with Millipore water followed by methanol and dried at 60˚C. This method was similar to the one employed by Toussaint and Luner [22]. FTIR spectrum of the cellulose

film was taken and it agrees well with the spectrum taken from the microgranula cellulose sample obtained from Aldrich (Figure 1).

AKD Sizing of cellulose films and filter paper

Cellulose films were sized for two different sizing levels using AKD-heptane solutions of two concentrations (0.2% and 0.6% (w/w)). Sizing was performed by slowly dipping glass slides into an AKD-heptane solution and slowly pulling them out of the solution. These slides were then heat treated in an oven at 105°C for 20 minutes.

Whatman #1 filter paper sheets were calendered by passing the sheet once through the nip of a laboratory calendar (Hunt and Moscrop). The cylinder surface temperature, measured using a thermocouple, was 150°C and the line pressure was set at 80 kNm^{-1}. sizing of the calendered filter paper sheets was performed following the same method described elsewhere [18]. The sized and calendered filter paper was used for the underwater AFM study.

Drop generation and image capturing for the drop impact analysis

An OCAH-230 apparatus (Dataphysics, Germany) was used to conduct the drop impact study. This apparatus has a computer controlled liquid drop dispensing syringe pump and a high-speed camera capable of 360 fps. A syringe with a flat-tipped stainless steel needle (o.d. = 0.31 mm) was fitted to the syringe pump, and a dispensing speed of 0.31 mL/s was programmed. The drop impact velocity was controlled by varying the height of the needle tip above the substrate surface. It was realized that a systematic error in drop velocity calculation was unavoidable, as the distance between the tip and the substrate was used. This is because that it is difficult to precisely determine the centre of mass of the drop immediately before its releasing using the present experimental set up. However, the error generated this way was expected to be constant, as the drop volume had been well controlled.

The high-speed camera captured the images of drop dispensing and impaction on the substrate. The camera was triggered by setting the software trigger line on the monitor just above the substrate surface. The data file was then analyzed using SCA20 software (Dataphysics). The water drop base diameter change during the impaction was calculated using a macro program written for the Image-Pro Plus software.

Surface energy calculation and drop impact modeling considerations

Surface energy calculation from contact angle data

Although the liquid drop impact process is significantly affected by liquid-solid interactions, the work of adhesion between the liquid drop and solid substrate in the impact process has not been considered in most previous studies [2,23]. Some authors used only the liquid properties and the drop kinetic energies to predict the impact results [2]. However, it is realized that the solid surface properties and the liquid-solid interactions play important roles in the liquid drop impaction on solid surfaces. This is particularly true to inkjet printing on complicated surfaces such as a sized paper. To facilitate the discussion of the results, a basic review of solid surface chemistry characterization and models of liquid impact on solid surfaces are presented below.

Terms of surface free energy, surface energy and surface tension will be used interchangeably.

Contact angle methods are indirect methods for measuring surface energetic of a solid sample. These methods rely on measurements of interactions between the liquid probes and the solid sample of interest. A common approach adopted in various mathematical models for calculating the components of surface energy is to first calculate the work of adhesion (W_a) between the solid surface and liquid probes [18,24].

$$W_a = \gamma_{lv}(1+\cos\theta) \tag{1}$$

where γ_{lv} is the surface tension of the liquid and θ is the equilibrium contact angle between the liquid and the solid. The concept of work of adhesion introduced by Dupre can be written as:

$$W_a = \gamma_{sv} + \gamma_{lv} - \gamma_{sl} \tag{2}$$

where γ_{sl} and γ_{sv} are the solid-liquid and solid-vapour interfacial free energies, respectively (in many situations where the liquid vapour pressures are low, γ_{sv} can be seen as the surface energy of the solid). Equation (1) can be obtained from equation (2) by substituting the Young's equation (eq. (3)).

$$\gamma_{sv} = \gamma_{sl} + \gamma_{lv}\cos\theta \tag{3}$$

There are several approaches to treat solid surface free energy, but the commonly used approach is to express the surface free energy as the sum of two components of intermolecular interactions which are due to the dispersion forces (γ^d) and the polar (e.g., hydrogen bonding) forces (γ^p):

$$\gamma = \gamma^d + \gamma^p \tag{4}$$

Fowkes [24] proposed "the geometric mean" rule to calculate the interfacial tension between phases 1 and 2. This rule was based on the assumption that only the dispersion components can be modeled using the geometric mean rule:

$$\gamma_{12} = \gamma_1 + \gamma_2 - 2\sqrt{\gamma_1^d \gamma_2^d} \tag{5}$$

However the most interfacial interactions in reality consist of both dispersion and polar contributions. Hence Owens and Wendt [25] extended the original geometric mean rule as follows.

$$\gamma_{12} = \gamma_1 + \gamma_2 - 2\sqrt{\gamma_1^d \gamma_2^d} - 2\sqrt{\gamma_1^p \gamma_2^p} \tag{6}$$

Combining equations (1), (2) and (6) and taking phases 1 and 2 as a solid and a liquid, the following working equation can be obtained:

$$W_a = \gamma_{lv}(1+\cos\theta) = 2\left(\sqrt{\gamma^d_{sv}\gamma^d_{lv}} + \sqrt{\gamma^p_{sv}\gamma^p_{lv}}\right) \quad (7)$$

The dispersion and polar components of surface tension for many liquids are known. Since there are two unknowns (γ^d_{sv} and γ^p_{sv}) in equation (7), one can calculate γ^d_{sv} and γ^p_{sv} by adopting a "two-liquid" experimental approach [24].

Further theoretical and practical considerations on work of adhesion

It is difficult to measure the work of adhesion between an aqueous liquid and a paper surface, even if the paper was sized and a stable apparent contact angle could be determined. Some researchers reported the surface energy data for sized papers using the contact angle methods [13,26,27], their results suggested that the heavily sized paper surfaces were similar to a hydrophobic polymer surface such as Telfon or polyethylene in that the polar component of the heavily sized paper was zero [13,26,27]. Some authors [26] used their results to justify the possible total coverage of the cellulose surface by the sizing chemical (AKD).

A problem of this approach was that the work of adhesion between water and paper or cellulose fibres could not be easily measured by contact angle methods. Shen *et al*. [18] showed that even though contact angle calculation predicted that there was no polar interaction between heavily sized paper samples and water, strong Lewis acid and base characteristics of paper surface could still be detected using other method (e.g. inverse gas chromatography). Although sizing was found to have reduced the Lewis acid and base components of the paper or cellulose fibre, these components were reduce only marginally and were still able to interact with a contacting liquid [18].

Many literature results [18,28,29] either suggested or implied that water or other polar liquids were able to have strong polar interactions with sized paper, even though water does not appear to spread on strongly sized paper surfaces. Fowkes [24] proposed that the work of adhesion contribution by the Lewis acid-base interactions could be written as

$$W_a^{AB} = fN(-\Delta H^{AB}) \quad (8)$$

where ΔH^{AB} is the molar enthalpy of acid-base adduct formation, N is the number of moles of interacting functional groups per unit area on the solid surface, and f is a conversion factor to correct enthalpy values to free energy values [19]. Equation (8) fits the situation of liquid – paper interaction well, as some literature results support the view that the surface of a heavily sized paper was not fully covered by a monolayer of sizing chemical and those uncovered hydroxyl groups of cellulose should be able to interact with water [18,28-30].

Modeling of maximum spreading

Figure 2 shows schematically the four stages of an aqueous liquid impact on a hydrophobic solid surface, as was summarized by Park *et al*. [1].

The aim of most of the modeling work was to predict the maximum spreading diameter of the drop at the impact. These models generally considered the relative magnitudes of energies of the liquid drop (kinetic, interfacial and viscous dissipation during the forces spreading and retraction) [6] and the energy conservation [1,2] of states

1 and 2. The Reynolds (*Re*) and the Weber numbers (*We*) were used as parameters to empirically correlate the maximum drop spreading diameters obtained experimentally with the theoretical models. The *Re* and *We* are defined as follow, they are dimensionless parameters that provide comparisons of the kinetic and the viscosity dissipation energies, and the kinetic and the surface energy of the drop, respectively.

$$Re = \frac{\rho u d}{\mu} \tag{9}$$

$$We = \frac{\rho d u^2}{\gamma_{lv}} \tag{10}$$

where ρ is the liquid density, u is the impact velocity, d is the liquid drop diameter and μ is the viscosity of the liquid. When kinetic energy is large enough to overpower the viscous force (i.e. large *Re*), the drop will spread more extensively upon impaction. When *We* is small, the surface tension dominates the behaviour of the drop and the drop tends to keep its spherical shape provided that no wetting takes place.

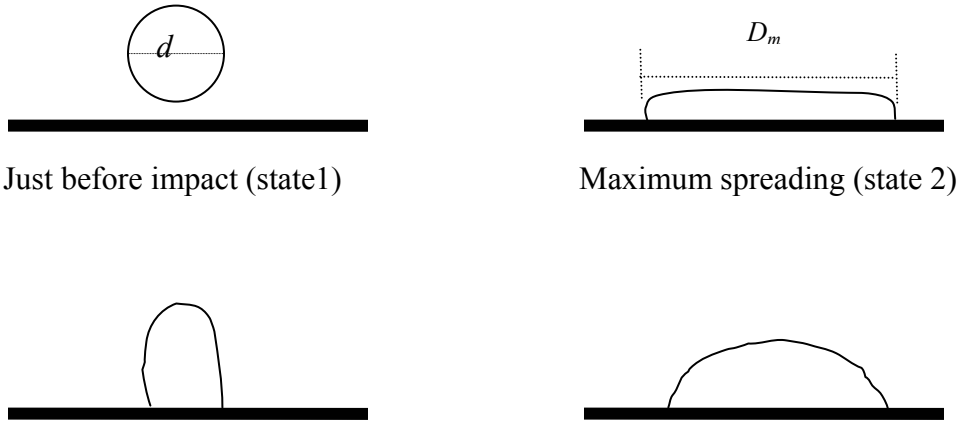

Figure 2. A schematic of the four stages of an aqueous liquid drop impact on a hydrophobic solid surface.

Early models for predicting the maximum drop spreading ratio, D_m^* (the ratio of drop diameter at state 2 (D_m) and the spherical drop diameter (d) at state 1, Figure 2), are based on the energy conservation [1,5,6]. It was assumed that the kinetic energy at maximum spreading is zero and the drop volume is constant. The energy conservation equation for states 1 and 2 was therefore proposed as follow:

$$KE^1 + SE_{lv}^1 + SE_{sv}^1 = KE^2 + SE_{lv}^2 + SE_{sl}^2 + VE^2 \tag{11}$$

where KE and SE denote kinetic and surface free energies, respectively. Superscripts 1 and 2 represents the impact stages 1 and 2, respectively, as shown in Figure 2, and *VE* is the viscously dissipated energy as the drop deforms from state 1 to state 2. By assuming the drop shape at the maximum spreading (state 2) being cylindrical [2] and spherical [1], Mao *et al*. [2] and Park et al. [1] proposed their equations for the prediction of maximum drop spreading at the drop impaction. Of course, the assumption on drop shape was not the only difference between the models proposed by these authors. Park *et al*. [1] introduced more mathematical considerations to accommodate the viscous dissipation in the energy balance for a special case, i.e. at zero impacting velocity. They argued that a liquid drop would change from a full spherical shape to a hemispherical shape when it contacts the solid surface. Viscous dissipation must be considered at the initial drop velocity is zero [1].

Park *et al*. [1] further explored the correlation between the apparent work of adhesion (W_a) calculated from the equilibrium contact angle values and the minimum diameter of the solid/water drop contact area, D_{min}, at the maximum drop recoil. Their correlation showed that D_{min} was much smaller when the W_a was low. In other words, D_{min} was much smaller if the solid surface was hydrophobic. Although Park *et al*. [1] showed that their model offered reasonably good correlations between the D_{min} and the W_a, it will be shown in this study that their model failed to provide useful correlation when paper was used as a substrate.

Since liquid drop recoil is an important part of the liquid drop impaction process, it is necessary that the drop recoil process be investigated as thoroughly as the process of the forced drop spreading. A good knowledge on the drop recoil is essential to the modeling work of ink inkjet droplet amalgamation after being printed on the surface of the substrate, and the ink droplet amalgamation after hitting the substrate is a factor that serious compromises the print quality [12].

Results and discussion

The maximum forced spreading of water drops impacting on various macroscopically smooth and a commercial paper surfaces

Apparent equilibrium contact angle values for diiodomethane and water on various solid surfaces are listed in Table 2. On the known high surface energy substrates such as glass and cellulose film, the contact angle values are very low.

Table 2: Contact angles between probe liquids and substrates

	Equilibrium Contact Angles (°)					
	Glass	Teflon	Cellulose	0.2%AKD-Cellulose	0.6%AKD-Cellulose	Reflex Copy Paper
Water	14.2	109.2	25	57.9	101.2	119.8
Diiodomethane	40.8	61.2	47.5	58.7	69.9	41.2

On the known low surface energy substrate, Teflon, the water contact angle is high. The contact angle for diiodomethane on Teflon surface was also higher than those on

other surfaces. Sizing of the cellulose films with AKD caused substantial increases in contact angles for both liquid probes. The lightly sized cellulose film was still partially wettable by water (equilibrium contact angle < 90˚) and this may be because that at this sizing level AKD only covered a fraction of the surface. In contrast to this, the heavily sized cellulose film (0.6% AKD) showed a non-wetting character. The contact angle between this surface and water drop (101.2˚) was close to the value reported for water on AKD wax, which was 109˚ [6]. This suggests that at this sizing level AKD coverage of the surface was close to the full coverage. The Reflex copy paper has a large apparent equilibrium contact angle with water (119.8˚). This contact angle was found to be very stable and there was no sign of water absorption by the sheet over 5 minutes.

Figure 3 illustrates the shapes of water drops at the maximum forced spreading upon impact on various solid surfaces. The most feature in Figure 3 is that the impacting contact angle for water on hydrophilic surfaces are very small, whereas for the less hydrophilic surface (such as the lightly sized cellulose film surface) and hydrophobic surfaces the impacting contact angles are greater than 90˚.

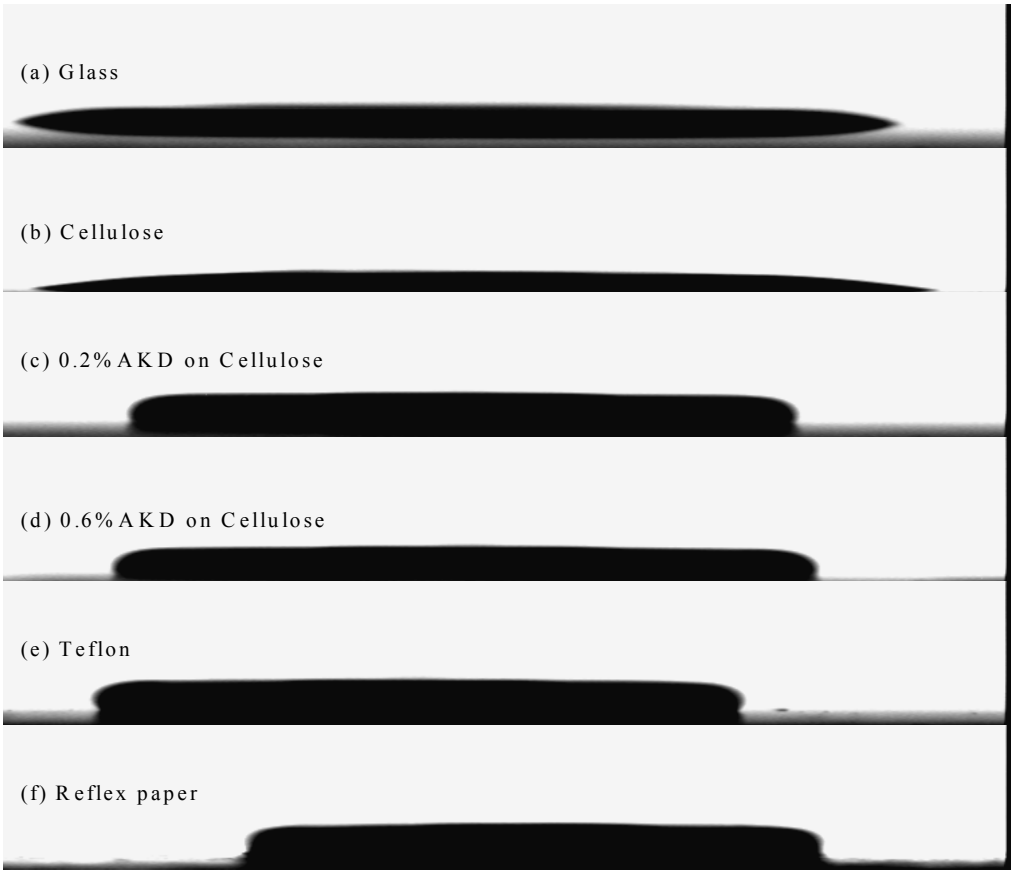

Figure 3. Water drop shapes on various substrates at the maximum forced spreading upon impact (impact velocity = 1 m/s).

Apparently, it is reasonable to assume that the shapes of the water drop at the maximum forced spreading on the lightly sized cellulose surface and other strongly hydrophobic surfaces are cylindrical, as suggested by Mao *et al*. [2] and Asai *et al*. [6].

However, for hydrophilic surfaces such as glass and cellulose film, it is less convincing to assume that the drop shapes are spherical, as suggested by Park et al. [1]. Figures 3 (a) and 3 (b) show that the centre region of the spread drop on hydrophilic surfaces is flat and this is expected to cause some error in the modeling. However, if the drop impact velocity is low, or if the contact angle at the maximum spreading is small, it is likely that the error associated with spherical assumption would also be small and the drop shape may be more accurately described by the spherical assumption than the cylindrical assumption.

Table 3 lists the maximum forced spreading ratios for water drops on various substrates obtained experimentally and using Park's model [1]. For all macroscopically smooth and impervious samples, this model exhibited a discrepancy ranging from 1% to 25%. There are few trends worth mentioning. First, the model by Park *et al*. [1] overestimated the D_m* for all impervious hydrophobic and hydrophilic at all impact velocities. Second, this model appears to give better prediction to drop impaction on smooth and impervious hydrophilic surface (i.e. glass and cellulose film). Third, the model always underestimate D_m* of copy paper and the discrepancy is about 25%. An analysis of the source of the discrepancy associated with the model was not pursued, as it was not the major focus of this study. However, the assumptions of the solid surface being topographically and chemically ideal could be responsible for introducing discrepancies between the experimental and the calculated results.

Table 3 Comparison of the maximum spreading ratios of water drops impacting various substrates with the model prediction of Park *et al*. [1]

Substrate	Dimensionless numbers	Impact Velocity (m/s)	Experimental data (D_m^*)	Model by Park et al. D_m^*
Glass	We=5	0.44	2.70	2.82
Cellulose	Re=997		2.44	2.75
0.2% AKD-Cellulose			1.67	2.08
Teflon			1.51	1.74
Copy Paper			2.23	1.66
Glass	We=16	0.77	2.97	3.24
Cellulose	Re=1744		3.12	3.17
0.2% AKD-Cellulose			2.32	2.74
Teflon			1.86	2.17
Copy Paper			2.76	2.10
Glass	We=28	1.00	3.15	3.46
Cellulose	Re=2265		3.13	3.39
0.2% AKD-Cellulose			2.54	3.01
Teflon			2.16	2.46
Copy Paper			3.31	2.38

The model by Park *et al*. [1] failed to give sensible predictions to drop impact on the copy paper surface. As was mentioned earlier, it is very difficult to model or measure the surface energy of a paper surface. It is therefore not surprising that the model by Park *et al*. [1] was unable to predict the relationship between D_m* and the work of adhesion between paper and water drop, either. More discussion will be offered in a latter section.

The maximum water drop recoil from hydrophobic surfaces after the forced spreading

Two macroscopically smooth hydrophobic surfaces, Teflon and polyethylene (PE), were used to demonstrate the recoil of water drops from hydrophobic surfaces. Water drop impact experiments were conducted at the drop velocity of 0.77 m/s. Figures 4 and 5 show statuses of the drops at (a) maximum forced spreading, (b) maximum recoil and (c) after reached equilibrium.

The water drop recoil from Teflon and PE surfaces shows similar behaviour. At the moment of maximum forced spreading, both surfaces were not wetted by water and had apparent contact angles at this state of greater than 90˚. Due to the lighting problem, the image in Figure 4 (a) is less clear. However, it still shows that the contact angle being greater than 90˚. Images in Figures 4 (a) and 5 (a) are in good agreement with the images reported by Park *et al*. [1] of the water drop impacted on Teflon surface.

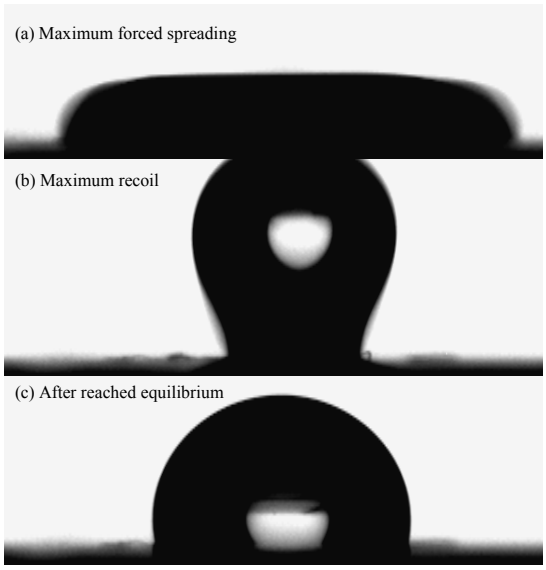

Figure 4. A water drop impaction on a Teflon surface at a velocity of 0.77 m/s: (a) Maximum forced spreading, (b) maximum recoil and (c) after reached equilibrium.

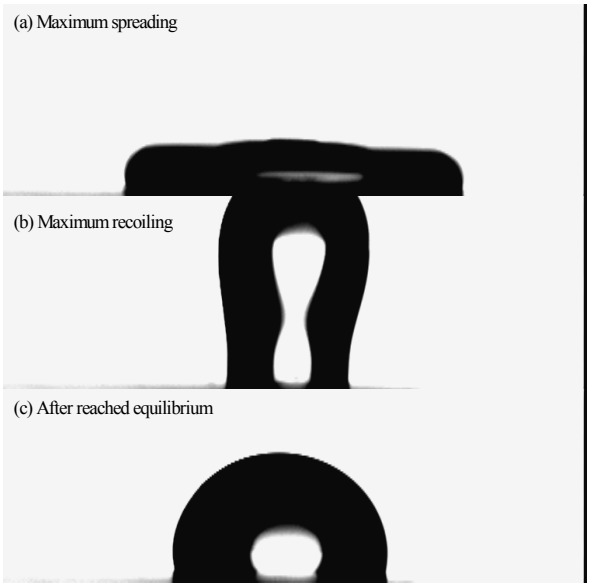

Figure 5. A water drop impaction on a PE surface at a velocity of 0.77 m/s: (a) Maximum forced spreading, (b) maximum recoil and (c) after reached equilibrium.

At the maximum forced spreading, some energy is lost due to the forced flow of the liquid [1,2,6]. Rest of the energy is converted into surface energy and interfacial energy, as described in equation (11). The pressure at the rim of the spread drop is the highest and points inward to the centre of the drop. It may be possible to estimate this pressure if

clear images (like that in Figure 3 (e)) can be obtained. On a highly hydrophobic surface, the Laplace pressure may then be estimated as:

$$\Delta P \approx 2\gamma\left(\frac{1}{D_m}+\frac{1}{t}\right) \tag{12}$$

where ΔP is the inward-pointing pressure exerted by the curved liquid surface, γ is the water surface tension, D_m is the diameter of the drop at the maximum forced spreading, $2(1/t)$ is the curvature of the rim of the drop shown in the image (Figure 3 (e)). The determination of this curvature may not be easy. However, in the extreme case where the contact angle at the maximum spreading is 180˚, t becomes the thickness of the flattened drop and the pressure can be calculated.

Table 4: Solid surface free energies (mJ/m^2) and work of adhesion (mJ/m^2)

Surface	Surface Energy	Polar Component	Dispersive Component	Work of Adhesion*
Glass	68.5	41.0	27.5	143.2
Teflon	24.6	0.0	24.6	48.8
PE	35.3	30.1	5.2	82.8
Cellulose	66.3	35.1	31.2	138.6
0.2%AKD-Cellulose	45.1	19.0	26.1	111.3
0.6%AKD-Cellulose	16.2	4.0	12.3	58.6
Copy Paper	49.5	4.0	45.5	36.6

This pressure is the driving force in the drop recoil. Since the work of cohesion of water ($W_c = 2\gamma_{water}$ = 144 mJ/m^2) is much higher than the works of adhesion for water/Teflon (48.8 mJ/m^2 , Table 4) and for water/PE (82.8 mJ/m^2, Table 4), the cohesion of water overcame the works of adhesion between water and these surfaces when water drop recoils. The water/Teflon interface generated at the maximum forced spreading could not be maintained during the recoil phase. As a result, the water drop recoils strongly from all hydrophobic surfaces. Mao *et al*. [2] and Parker *et al*. [1] also observed that water drop recoiled back strongly from the surfaces of paraffin and Teflon, respectively. It is worth noting that both the lightly and highly sized cellulose films (0.6% AKD) behave in the same manner as a strongly hydrophobic surface in the maximum recoil phase (Table 5).

The maximum water drop recoil from hydrophilic surfaces after the forced spreading

Two macroscopically smooth hydrophilic surfaces, glass and cellulose film on glass slide, were used to demonstrate the recoil of water drops from hydrophilic surfaces. Water drop impact experiments were conducted at the drop velocity of 0.77 m/s. Figures 6 and 7 show statuses of the drops at (a) maximum forced spreading, (b) maximum recoil and (c) after reached equilibrium.

The water drop recoils from glass and cellulose surfaces in a similar manner. At the maximum forced spreading, both surfaces were wetted by water and apparent contact angles at this state were much smaller than 90˚. Because the rim curvatures of the water drop on glass and cellulose surfaces were much smaller than those on the hydrophobic

surfaces, the inward-pointing pressure was much weaker. As a result, water drops only showed very weak recoils from the hydrophilic surfaces after impaction.

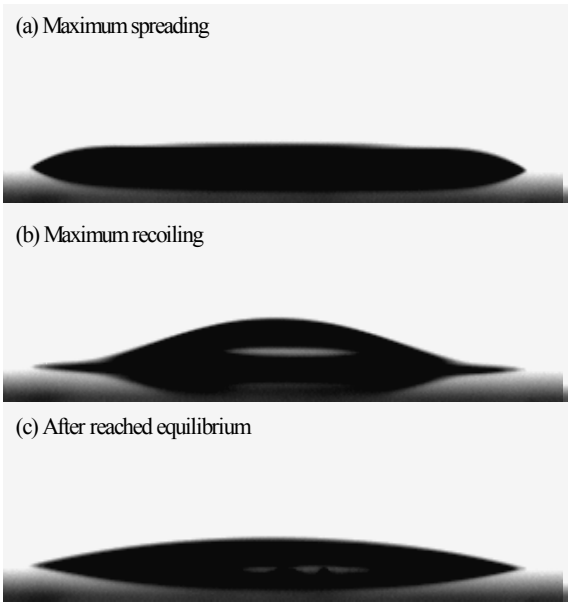

Figure 6. A water drop impaction on a glass surface at a velocity of 0.77 m/s:(a) Maximum forced spreading, (b) maximum recoil and (c) after reached equilibrium.

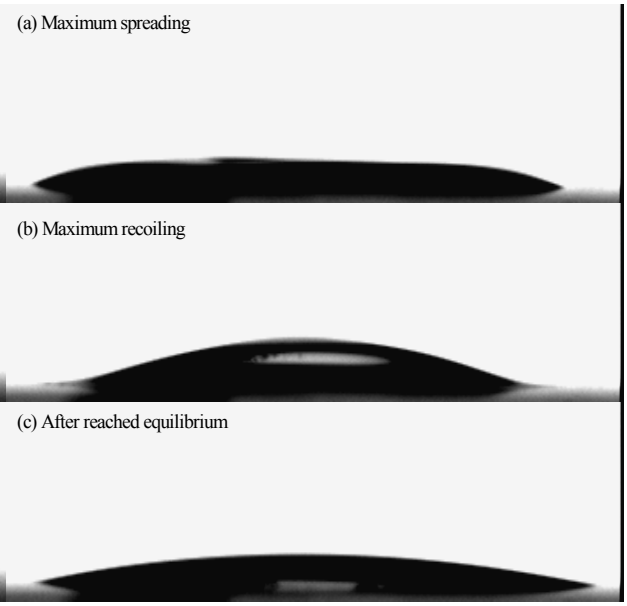

Figure 7. A water drop impaction on the surface of a cellulose film coated on glass slide at a velocity of 0.77 m/s: (a) Maximum forced spreading, (b) maximum recoil and (c) after reached equilibrium.

Another reason for water drop to have weak recoil from these hydrophilic surfaces was that strong water-substrate adhesion was established. The works of adhesion between water-glass and water-cellulose calculated using equation (7) (see Table 3) show that they are of the same magnitude as the work of cohesion of water ($W_c = 2\gamma_{water} = 144$ mJ/m^2). The immediate wetting of these substrates by water upon impaction suggests that the adhesion between water and the glass and cellulose surfaces has established in the time scale of the impaction.

The comparison of the works of adhesion between water and these hydrophilic substrates and the work of cohesion of water can also explain the observed phenomenon that the interface areas between these substrates and water established at the maximum forced spreading were not reduced at the maximum recoil.

The maximum water drop recoil from a sized paper surface after the forced spreading

A sized commercial copy paper was used to demonstrate the recoil of a water drop from a sized paper surface. Water drop impact experiments were conducted at the drop velocity of 0.77 m/s. Figure 8 shows statuses of the drop at (a) maximum forced spreading, (b) maximum recoil and (c) after reached equilibrium.

Table 5 Contact angles and droplet diameter at different impact states

	Static *CA*	CA_{im}	D_m	D_{min}	D_e
Water-Glass					
0.44m/s	14.2	12.2	5.5	5.3	6.3
0.77m/s	14.2	10.1	6.0	6.0	6.6
1.0m/s	14.2	9.0	6.4	5.9	6.3
Water-Cellulose					
0.44m/s	25.0	18.1	4.9	4.4	5.4
0.77m/s	25.0	12.8	6.3	6.2	6.6
1.0m/s	25.0	11.5	6.3	6.2	6.4
Water-0.2%AKD+Cellulose					
0.44m/s	57.9	74.5	3.4	3.3	3.3
0.77m/s	57.9	54.9	4.7	4.5	4.2
1.0m/s	57.9	44.4	5.1	4.5	4.3
Water-0.6%AKD+Cellulose					
0.44m/s	101.2	102.8	3.4	2.2	2.7
0.77m/s	101.2	107.7	*droplet divded to two part at*		
1.0m/s	101.2	106.2	*the maximum rebound*		
Water-Teflon					
0.44m/s	109.2	104.8	3.1	2.2	2.5
0.77m/s	109.2	103.2	3.8	1.3	2.5
1.0m/s	109.2	103.7	4.4	1.7	2.5
Water-Reflex					
0.44m/s	119.8	87.6	4.5	4.3	4.5
0.77m/s	119.8	60.6	5.6	5.3	5.6
1.0m/s	119.8	41.3	6.7	6.1	6.6

Static *CA =contact angle obtained by delivering at minimum possible('zero') velocity*

CA_{im} *= contact angle at the state 4(equlibrium)*

D_m *=maximum spreading diameter*

D_{min} *= diameter at maximum rebound*

D_e *=diameter at the equlibrium(approx. 5sec after impact)*

Compared with macroscopically hydrophobic and hydrophilic surfaces, the sized paper surface shows interesting behaviour when a water drop impacts on it. When a water drop hit the sized paper surface and was forced to spread, the contact angle between water and the paper at the maximum forced spreading was greater than 90˚ (figure 8 (a)). The rim of the water drop has a large curvature, which generates a strong inward-pointing pressure. At this stage the sized paper showed typical characteristics of a hydrophobic surface. The inward-pointing pressure causes the water drop to strongly recoil after the impaction (Figure 8 (b)). When the drop began to recoil, since the water-paper contact line was pinned, the drop started to behave differently to a hydrophobic surface (see Figures 5 (b), 6 (b) and 8 (b)). Since the water-paper contact line did not retreat significantly during the recoil, the apparent water-paper interface did not change after reached to its maximum size in the forced spreading phase. In this respect, the sized paper surface behaved somewhat similar to a hydrophilic surface. As shown in Figures 6 and 7, a hydrophilic surface only causes very weak water drop recoil. However, since sized paper showed a typical hydrophobic property in the forced spreading phase, water drop recoil from the paper surface was much stronger than from a hydrophilic surface, although soon after the drop recoil phase started, the sized paper behaved like a hydrophilic surface.

Such a switch of properties of sized paper during the water drop impact suggests that paper, even strongly sized paper, should not be simply regarded as a hydrophobic surface. Whilst the pinning of the water-paper contact line can offer an explanation to this phenomenon, what can be said in addition is that the adhesion between water and the sized paper was established immediately after the impact of the water drop. Such an adhesion is likely to be rather strong, even though the apparent static contact angle between water and the sized paper was quite large (Table 2) and the apparent work of adhesion calculated using those contact angle data was very low (Table 4). More discussion on the work of adhesion will be offered in later sections.

Surface roughness of the paper is also likely to have certain influence on the water drop recoil, since the roughness of a surface contributes to the pinning of the liquid-solid contact line [31]. However, surface chemical heterogeneity is known to also contribute to the pinning of the contact line [32]. Figure 9 shows the water drop impaction and recoil process on a lightly sized cellulose film surface. At the impact velocity 0.77 m/s, the drop recoiled in a very similar fashion as it did from a sized paper surface in that there was little or no loss of the drop-substrate interface area at the maximum drop recoil. Interestingly though, in the process of reaching to the equilibrium contact angle, the apparent interface area between the water drop and the film reduced slightly. The water drop impaction behaviour at other velocities is presented in Table 5. This behaviour may be attributable to the fact that cellulose film was much smoother than the paper surface.

Despite that the surface roughness of the lightly sized cellulose film and the sized paper is different, the behaviour of water drop recoil from these surfaces are similar. This suggests that forced wetting and the immediate establishment of adhesion are the dominant factors contributing to switch of the water drop behaviour at the impact and recoil process.

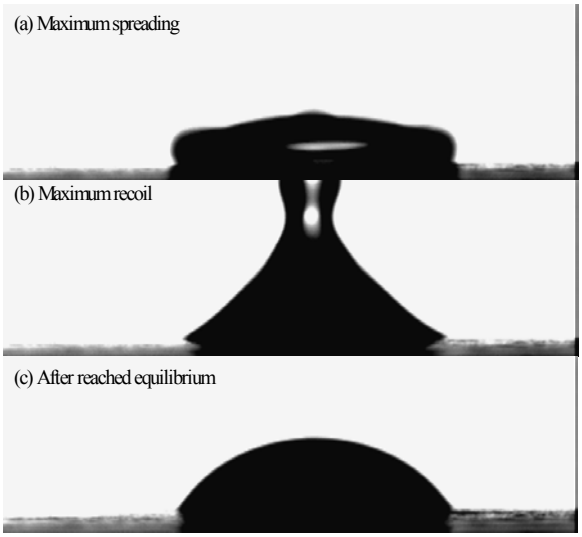

Figure 8. A water drop impaction on the surface of a copy paper at a velocity of 0.77 m/s: (a) Maximum forced spreading, (b) maximum recoil and (c) after reached equilibrium.

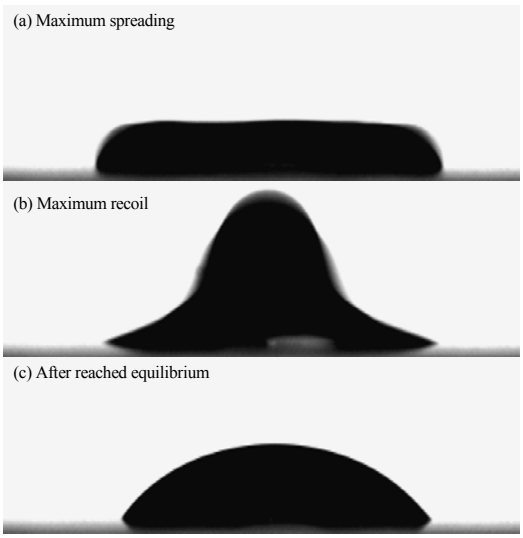

Figure 9. A water drop impaction on the surface of the lightly sized cellulose film surface (0.2 % AKD) at the velocity of 0.77 m/s: (a) Maximum forced spreading, (b) maximum recoil and (c) after reached equilibrium.

The adhesion of water with sized paper and fibre surface

Park *et al.* [1] used a correlation between D_{min}/d (d is the diameter of the liquid drop before impact, as shown in Figure 2) and the normalized work of adhesion (W_a/γ_{lv} = (1+cosθ)) to demonstrate a correlation between the liquid/substrate adhesion and the liquid drop recoil. Since the work of adhesion is a thermodynamic quantity, the contact angle they used for the correlation was the static apparent contact angle. Their correlation showed that, for smooth and impervious surfaces (Teflon, glass and HMDS coated silicon wafer), as the normalized work of adhesion (1+cosθ) increased, the D_{min}/d also increased. Their results therefore suggested that a strong work of adhesion between the liquid and the substrate would hamper the liquid drop recoil. This method of correlation was used to fit the data obtained from the present work (Figure 10).

Figure 10 shows that, whereas correlations between (D_{min}/d) and the normalized W_a for water on glass, cellulose film, lightly sized cellulose film and Teflon followed a similar trend to those reported by Park *et al*. [1], the recoil of water drop from copy paper surface fell totally outside the prediction of this correlation (Figure 10).

This rather interesting behaviour of water-paper interaction suggests that care must be taken if one attempts to use an existing model for ideal model surfaces to predict the spreading and recoil behavior of a water drop on paper surface. The followings may be two of the major reasons why paper behaves so differently to other substrates.

First, it is not easy (if not impossible) to obtain a thermodynamically meaningful contact angle value from a paper surface. The measured value of the apparent contact angle for a liquid on a solid surface can be strongly influenced by paper surface roughness. Shen *et al.* [18] showed that the work of adhesion calculated using apparent

static contact angle data on sized paper surface were not reliable. Most likely, the contact angle method will underestimate the work of adhesion.

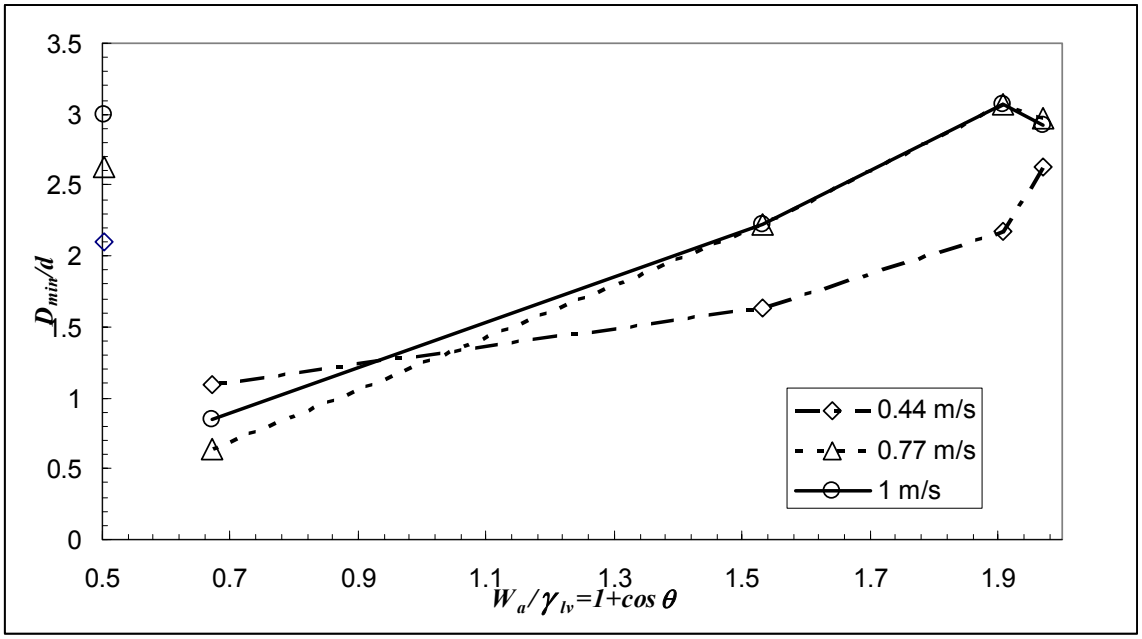

Figure 10. The correlation between the normalized work of adhesion (W_a/γ_{lv}) and the minimum spreading ratio (D_{min}/d). A, B, C, D and E are cellulose film, glass, lightly sized cellulose film (0.2 g/L, see experimental section), Teflon and copy paper, respectively.

Second, sized papers usually show a substantial contact angle hysteresis. Early studies by Hodgson and Berg [33] showed that, while the advancing contact angles of heavy sized cellulose fibers with water ranged from 120 – 140˚, the receding contact angles were always 0˚. von Bahr *et al*. [8] also noted that the receding contact angle for water on a heavy sized paper was very low. These observations suggested that a sized paper, although shows a high degree of resistance to water wetting and penetration, adheres well with water when it is in contact with water. Shen *et al*. [18] showed that the work of adhesion between water and sized paper calculated using data obtained from inverse gas chromatography (IGC) was much higher than that calculated using the apparent static contact angle data. Whilst the contact angle results failed to reveal any hydrogen bonding interactions between water and strongly sized papers [13,18,26], IGC results revealed that there was a strong hydrogen bonding capability for sized paper surfaces [18]. Their results suggested that molecules of the sizing agent did not totally cover the surface of the paper, cutting off all hydrogen bonding interactions between water and the paper surface. Instead, the distribution of the sizing agent on the surface of the paper is likely to be only partial. However, the distribution of the sizing chemical on fibre surface is unknown. It is likely, though, that the distribution may not be uniform at a molecular level. This allows the interaction (and therefore adhesion) to be established when water is in contact with the paper surface. In fact, water-paper interactions under this condition can be better described by equation (8). This analysis agrees with the research reported by Strom *et al*. [30] that the coverage of AKD on a sized paper surface is far less than a complete mono-layer.

The above analysis allows the following picture to be formed: The wetting condition at the water-paper contact line is very complicated, as there are areas which are not covered by the sizing agent having very low contact angle, whereas areas that are covered by the sizing agent showing higher contact angle. This condition will allow pinning of the contact line to occur [18]. Although paper surface roughness certainly also contributes to the pinning [11], we argue that the surface heterogeneity also strongly contributes to the pinning. The strong adhesion of water on areas of cellulose fibre surface that are not covered by AKD is established. This will also allow water to penetrate into the fibre wall.

To further discuss the water-paper interaction, AFM was used to acquire images of a cellulose fibre on a heavily sized and calendered filter paper surface before and after it was brought in contact with water (Figure 11 (a) and (b)). A consideration in choosing the sized filter paper was that the influence of filler particle can be avoided. Since the water drop can be held stably on the sized paper surface, an AFM image was obtained under the drop of water (Figure 11 (b)). However, the degree of difficulty in performing *in situ* AFM imaging on the same fibre after introducing water hampered the chance for collecting high quality AFM image. Nevertheless, we believe that these images contain some information that supports the strong interaction between water and a strongly sized paper surface.

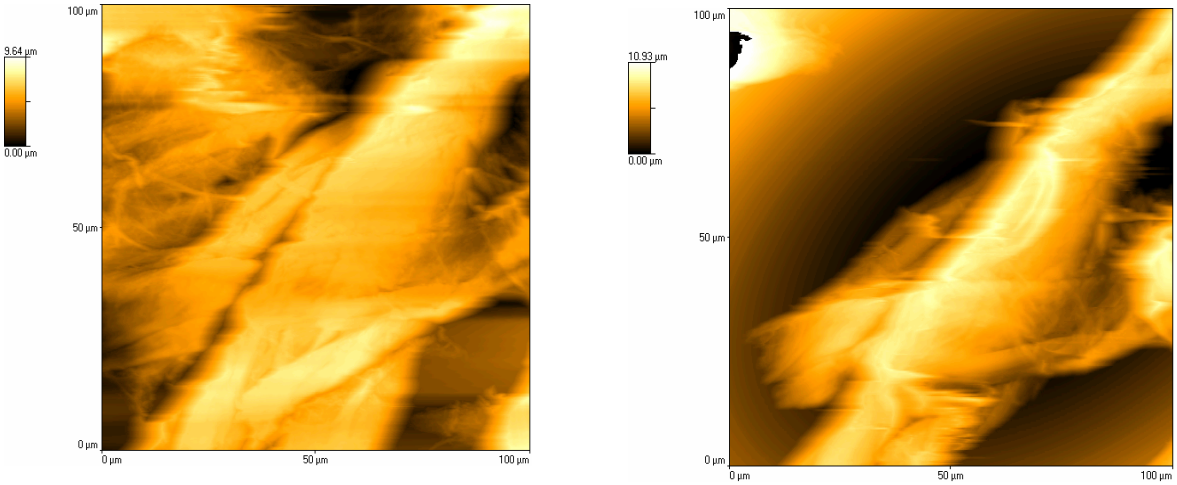

Figure 11. (a) AFM image of a cotton lint fibre on the surface of a strongly sized and calendered filter paper. (b) AFM image obtained under water of the same fibre.

The major feature of Figure 11 (a) is a thick and long cotton lint fibre laying diagonally across the figure. On the left side of the figure are other fibres at about the same height as the major fibre in the figure. Figure 11 (b) shows that after water was introduced, the major fibre in the figure appeared to be raised up. The most likely cause for such a change to occur was that water strongly interacts with the fibre, causing the fibre to swell. This interaction therefore leads to a relaxation of the fibre matrix. Unfortunately, attempts of recording scans of smaller scales were unsuccessful, because of the continuous swelling of the fibre.

Such a strong interaction between water and the heavily sized paper, however, cannot be correctly reflected by the contact angle and the work of adhesion value calculated from the contact angle for reasons given in an earlier section (see Table 4). The present AFM results once again showed that water can adhere strongly to the sized paper surface possibly through areas that are not covered by the domains of the sizing chemicals on the fibre surface. These results are in good agreement with the observation made by Roberts *et al*. [15] using confocal microscopy that water penetrates into the wall of strongly sized fibres after contact.

Implication of water impact behaviour on paper surface to inkjet printing

The advancement of inkjet printing technology allows the much smaller ink droplet to be delivered on to paper surface. At the same time the ink droplet delivering rate has increased significantly [34]. The development of specialty inkjet papers emphasizes the use of ink receptive coating. The coating layer must not only absorb the ink rapidly, but also be able to chemically anchor the dye molecules. On the other hand, however, normal uncoated but sized office papers are still being used in large quantity for inkjet printing.

A factor which has been demonstrated to be potentially detrimental to ink print quality is the ink droplet amalgamation after being printed on the paper surface. The ink droplet amalgamation obviously depends on the shortest distance between the printed dots (droplets) on the paper surface. Since the shortest distance between the printed dots on a paper surface is determined by the forced spreading of the ink droplet in the impaction phase and not affected by the process of drop recoil, the droplet amalgamation is most likely be only determined by the droplet impaction.

Print quality analysis of inkjet printed solid tone images on some uncoated but strongly sized and supercalender papers often reveal speckles of areas of ≤ 1 mm^2. It is possible that the surface conditions of the speckles are different from that of their surrounding areas. These areas might either have a higher sizing level (due to uneven size distribution) or have a greater smoothness or both. In this case the area of speckles would behave like the strongly sized cellulose films which strongly reject ink droplets.

It is a well observed phenomenon that applying a strong sizing only, without also applying other appropriate surface treatments to paper, can significantly increase the level of inkjet print mottle [35]. Observations from this study lend some support to this phenomenon. On a sized paper surface, ink droplets are likely to recoil quite strongly after impaction (see Figure 8 (b)), since in the impact phase the sized paper behaves like a hydrophobic surface. Such recoil could provide a chance for the ink droplets to redistribute before being absorbed into paper. Since the paper surface is microscopically rather rough, the impacting drops do not necessarily rebound perpendicularly to the paper surface all the time. This makes the redistribution of the droplets (before penetration) practically likely. The redistribution of the droplets may encourage the formation of small "reservoirs" on the paper surface; the subsequent penetration of ink in these reservoirs may be an enhancing factor to the formation of print mottle.

Conclusion

The impact of water drops on a solid substrate is highly dependent on the drop kinetic energy and the liquid-substrate interactions. Experiments conducted on the hydrophilic and hydrophobic model surfaces confirmed the following literature results. On a hydrophobic model surface, water drop spreads to the maximum diameter (D_m) under the force of impact and then retracts from the surface to a minimum diameter (D_{min}) which is smaller than D_m. On a hydrophilic model surface, water drop spreads to the maximum diameter, but it does not strongly retract from the surface. Therefore, for a hydrophilic model surface, $D_{min} \approx D_m$. Water drop impact on sized paper surface exhibits a switch of behaviour. At the moment of drop impact, the sized paper behaves like a hydrophobic surface. During the drop recoil, sized paper behaves like a hydrophilic surface. When the impacting drop reaches equilibrium, the sized paper again behaves like a hydrophobic surface, allowing no water penetration. When water is in contact with the sized paper surface, good adhesion between the water and the sized paper surface can be established in the time scale of the drop impaction. This adhesion prevents water to retract from the sized paper surface. The results from this study are relevant and useful to the understanding of inkjet ink droplets impaction on paper surface.

Acknowledgements

This work was carried out as part of the research program for the CRC Smart Print. Funding received from the Federal Government and the CRC program is gratefully acknowledged. One of us, Dr. Hailong Zhang, would like to gratefully acknowledge the financial support from BASF through the joint research project (No. 243-7249).

References

[1] H. Park, W.W. Carr, J. Zhu and J.F. Morris, Single drop impaction on a solid surface. *Fluid Mech. Trans. Phenomena*, 49 (2003) 2461 – 2471

[2] T. Mao, D.C.S. Kuhn and H. Tran, Spread and rebound of liquid droplets upon impact on flat surfaces. *AIChE J.* 43 (1997) 2169 – 2179

[3] J. Fukai, Y. Shiiba, T. Yamamoto, O. Miyataka, D. Poulikakos, C.M. Megaridis, and Z. Zhao, Wetting effects on the spreading of a liquid droplet colliding with a flat surface. *Phys. Fluids*, 7 (1995) 263

[4] J. Fukai, M. Tanaka, and O. Miyatake, Maximum Spreading of liquid droplets colliding with flat surfaces. *J. Chem. Eng. Japan*, 31 (1998) 456

[5] J. Fukai, Z. Zhao, D. Poulikakos, C.M. Megaridis and O. Miyatake, Modeling of the deformation of a liquid droplet impinging upon a flat surface. *Phys. Fluids*, 5 (1993) 2588

[6] A. Asai, M. Shioya, S. Hirasawa and T. Okazaki, Impact of an ink drop on paper. *J. Imaging Sci. Technol*. 37 (1993) 205 -207

[7] J. Heilmann, Measuring dynamic interactions between paper and microscale ink drops. *IS&T's NIP 17: International Conference on Digital Printing Technologies,* (2001). 735-738.

[8] M. von Bahr, F. Tiberg and V Yaminsky, Spreading dynamics of liquids and surfactant solutions on partially wettable hydrophobic substrates. *Colloids Surf. A*. 193 (2001) 85-96
[9] M. von Bahr, F. Tiberg and B.V. Zhmud, Spreading Dynamics of surfactant solutions. *Langmuir*, 15 (1999) 7069 – 7075
[10] M. Apel Paz, A. Marmur, Spreading of liquids on rough surfaces. *Colloids Surf. A*. 146 (1999) 273 – 279
[11] H. Modaressi and G. Garnier, Mechanism of wetting and absorption of water droplets on sized paper: Effects of chemical and physical heterogeneity. *Langmuir*, 18 (2002) 642 – 649
[12] R. Urquhart, Inkjet ink and paper interaction. *Australian Printer*, Sept (2004) 64
[13] M. von Bahr, PhD thesis, *Wetting and capillary flow of surfactant solutions and inks*, Lund University, Sweden, (2003)
[14] M.B. Lyne and J. Aspler, Ink-paper interactions in printing: a review. In *Colloids and Surface in reprographic technology*, pp. 385. M. Hair and K.D. Croucher (Eds). ACS Symposium series. No. 200, (1982)
[15] R. Roberts, Tim J. Senden, M.A. Knackstedt and M.B. Lyne, Spreading of aqueous liquids in unsized papers is by film flow. *J. Pulp Paper Sci*. 29 (2003) 123
[16] H. Yamazaki and U. Munakata, A liquid absorption model, in *Products of paper making, Trans. 10th Fundamental Res. Symp.* C.F. Baker (Ed.), p913 – 934, Oxford, (1993).
[18] W. Shen, Y. Filonenco, I.H. Parker, N. Brack and P. Pigram, Contact angle and surface energetics measurements of sized and unsized papers. *Colloids Surf. A*. 173 (2000) 117 – 126
[19] J.C. Berg, "Role of acid-base interactions in wetting and related phenomena" in *Wettability*, J.C. Berg (Ed.), p75 – 148. Marcel Dekker, NY, (1993)
[17] R. Roberts, Tim J. Senden and M.A. Knackstedt, 3D imaging of the spreading and penetration of aqueous liquids into unsized and sized papers. *5th International paper and coating symposium*, (2003) 303
[21] R.J. Good, "Contact angle, wettability and adhesion – a critical review" in *Contact angle, wettability and adhesion*, p3 – 36. K.L. Mittal (Ed.), Utrecht, The Netherlands, (1993)
[22] T. Onda, S. Shibuichi, N. Satoh and K. Tsujii, Super-water-repellent fractal surfaces. *Langnuir*, 12 (1996) 2125 – 2127
[23] L. Cheng, Dynamic spreading of drops impacting onto a solid surface, *Ind. Eng. Chem. Process Res. Dev*. 16 (1977) 192-197
[24] F.M. Fowkes and M.A. Mostafa, *Ind. Eng. Chem. Prod. Res. Dev*. 17 (1978) 3
[25] R.E. Johnson (Jr.) and R.H. Dettre, "Wetting of low energy surfaces" in *Wettability*, J.C. Berg (Ed.), p1 – 74. Marcel Dekker, NY, (1993)
[26] D.T. Quillin, D.F. Caulfield and J.A. Koutsky, Cellulose/polypropylene composites: the use of alkyl ketene dimer (AKD) and alkenyl succinic anhydride (ASA) sizes as compatibilizers. *Int. J. Polym. Mater.* 17 (1992) 215 – 227
[27] Y. Huang, D.J. Gardener, M. Chen and C.J. Biermann, Surface energetics and acid-base character of sized and unsized paper handsheets, *J. Adhesion Sci. Technol*. 9 (1995) 1403-1412

[28] W. Shen and I.H. Parker, "Surface composition and surface energetics of various eucalypt pulps", *Cellulose* 6 (1999) 41 – 55
[20] J. Roberts, in *Paper Chemistry*, Chapter 8, Blackie Academic & Professional, London, (1996)
[29] J.A. Bristow, The pore structure and sorption of liquids, in *Paper structure and properties*, J.A. Bristow Ed., p188. Marcell Dekker, (1986)
[30] G. Strom, G. Carlsson and M. Kiar, Bestimmung der alkyketendimer-verteilung in probeblattern mittels elektronenspektroskopic (ESCA). *Wochenblatt fur papierfabrikation*, 15 (1992) 606
[31] R. Dettre and R. Johnson, in *Contact angle, wettability and adhesion*, F.M. Fowkes Ed., pp. 136. ACS Series, No. 43, Washington D.C. (1964)
[32] P.G. de Gennes, Wetting: statics and dynamics, *Reviews of modern physics*, 57 (1985) 827 – 863
[33] K.T. Hodgson and J.C. Berg, Dynamic wettability properties of single wood pulp fibers and their relationship to absorbency, *Wood Fiber Sci*. 20 (1988) 3.
[34] H. Kipphan, Handbook of print media, p.711. Springer-Verlag, Germany, (2001)
[35] D.F. Varnell, Paper properties that influence ink-jet printing, *Pulp Paper Can*. 99 (1998) 37